Comparison of the Use of Liver Models for Predicting Drug Clearance Using *in Vitro* Kinetic Data from Hepatic Microsomes and Isolated Hepatocytes

Kiyomi Ito[1] and J. Brian Houston[1,2]

Received December 11, 2003; accepted February 5, 2004

Purpose. To compare three liver models (well-stirred, parallel tube, and dispersion) for the prediction of *in vivo* intrinsic clearance (CL_{int}), hepatic clearance (CL_h), and hepatic availability (F_h) of a wide range of drugs in the rat using *in vitro* data from two *in vitro* sources.

Methods. *In vitro* CL_{int} was obtained from studies using isolated rat hepatocytes (35 drugs) or rat liver microsomes (52 drugs) and used to predict *in vivo* CL_{int} using reported scaling factors, and subsequently CL_h and F_h were predicted based on the three liver models. In addition, *in vivo* CL_{int} values were calculated from the reported values of CL_h based on each of the three models.

Results. For all of the parameters, predictions from hepatocyte data were consistently more accurate than those from microsomal data. Comparison of *in vitro* and *in vivo* CL_{int} values demonstrated that the dispersion model and the parallel tube model were comparable and more accurate (less bias, more precise) than the well-stirred model. For CL_h and F_h prediction, the three models performed similarly.

Conclusions. Considering the statistics of the predictions for three liver models, the use of parallel tube model is recommended for the evaluation of *in vitro* CL_{int} values both from microsomes and hepatocytes. However, for the prediction of the *in vivo* drug (hepatic) clearance from *in vitro* data, as there are minimal differences between the models, the use of the well-stirred liver model is recommended.

KEY WORDS: dispersion model; hepatic clearance; intrinsic clearance; parallel tube model; well-stirred model.

INTRODUCTION

The use of *in vitro* data to make predictions of *in vivo* clearance is a well-accepted procedure (1,2) and both isolated hepatocytes and hepatic microsomes have been advocated as suitable sources of kinetic parameters (3). Kinetic parameters from either metabolite formation (V_{max} and K_m) or drug substrate depletion over time (clearance or half-life) can be used. Studies in rats have allowed the strategy to be validated as the use of this animal species, in contrast to human, allows consistency in both genetic components and environmental conditions and hence ensures the maximum degree of comparability between the experimental conditions applicable to *in vitro* and *in vivo* phases of the studies. The general strategy has two essential steps. The initial step converts units of *in vitro* data expressing the clearance parameter (intrinsic clearance, CL_{int}), in terms of total liver weight rather than the *in vitro* units of millions of cells or milligrams of microsomal protein. The second step incorporates other physiological processes such as blood flow and plasma protein binding, with the intrinsic metabolic stability of a drug to provide a whole liver parameter (hepatic clearance, CL_h).

Thus, the use of liver models is an essential step in the scaling process used to relate the clearances obtained *in vitro* to the *in vivo* situation. By allowing for drug concentration differences across the liver and accounting for physiological factors such as blood flow and plasma protein binding, the intrinsic metabolic stability of a drug can be integrated into a whole liver application. The most established models are the "well-stirred," parallel tube, and dispersion models of which the "well-stirred" model is most often used due to its mathematical simplicity rather than any superiority over the others; indeed, it is the least "physiological" in nature. To mimic the *in vivo* situation these models all assume that 1) the distribution into the liver is perfusion rate limited with no diffusion barriers, 2) only unbound drug crosses the cell membrane and occupies the enzyme site, and 3) there is a homogenous distribution of metabolic enzymes in the liver (3). However, different assumptions are made regarding the concentration gradient of drug within the liver; the "well-stirred" model assumes that the hepatic drug concentration is equal to the outflow concentration, the parallel tube model assumes it is equal to the logarithmic mean of inflow and outflow concentration, and the dispersion model assumes it shows axial dispersion analogous to packed-bed chemical reactor.

The aim of this study is to afford a comprehensive comparison of these three liver models to predict *in vivo* CL_{int}, CL_h, and hepatic availability (F_h) from rat *in vitro* data. Comparisons published previously have focused on a relatively small number of drugs (3–5). This investigation uses both literature and in-house *in vitro* data from rat microsomal and hepatocyte studies for 52 and 35 drugs, respectively, and data for rat hepatic clearance *in vivo* to create a substantial data set from which to make these comparisons. Rat rather than human data were used in order to 1) make use of available hepatocyte, in addition to microsomal *in vitro* data, and 2) avoid the additional confounding issues of interindividual variability seen both *in vitro* and *in vivo*.

MATERIALS AND METHODS

Data Collection

Table I shows the list of studied compounds (n = 59). *In vitro* intrinsic clearance (CL_{int}) in rats was obtained from published metabolic studies or studies performed in our laboratory using isolated rat hepatocytes (35 drugs) or rat liver microsomes (52 drugs). *In vivo* hepatic clearance (CL_h) in rats was also obtained from the literature or in our laboratory. Some of the compounds were also studied in rats treated with CYP inducers such as phenobarbital (PB), β-naphthoflavone (BNF), and dexamethasone (DEX), or an inhibitor aminobenzotriazole (ABT).

In vitro/In vivo Scaling

The units of *in vitro* CL_{int} values (μl/min per 10^6 cells or μl/min per mg microsomal protein) were converted to ml/min

[1] School of Pharmacy and Pharmaceutical Sciences, University of Manchester, Manchester M13 9PL, UK.

[2] To whom correspondence should be addressed. (e-mail: Brian.Houston@man.ac.uk)

0724-8741/04/0500-0785/0 © 2004 Plenum Publishing Corporation

Table I. *In vitro* CL_{int} and *In vivo* CL_h Values in Rats

Compound	*In vitro* CL_{int} Hepatocyte (μl/min/10^6 cells)	*In vitro* CL_{int} Microsomes (ml/min/mg protein)	*In vivo* CL_h (mm/min/SRW)	f_u	References
R-acenocoumarol	ND	11	0.33	0.012	3
S-acenocoumarol	ND	30	1.2	0.009	3
Alprenolol	36	80	24	1	6
Aminopyrine	4.1	6.6	2.0	1.0	6
Antipyrine	0.80	3.6	1.4	1	6
Bosentan	ND	40	14	0.02	7
Butylbarbitone	1.9	ND	1.2	0.6	6
Carbamazepine	ND	2.2	0.78	1	6
Diltiazem	ND	250	12	0.198	8
Dofetilide	ND	18	7.8	0.47	3
Ethoxybenzamide	1.3	4.5	2.2	0.5	6
Felodipine	ND	500	5.9	0.07	6
FK1052	ND	550	13	0.025	8
FK480	ND	130	8.6	0.016	8
Hexylbarbitone	21	ND	4.9	0.18	6
Imipramine	990	4500	22	0.107	6
Indinavir	ND	70	16	0.3	9,10
L-738,372	ND	4.3	3.8	1	11
Lignocaine	ND	200	24	1	6
Loxtidine	11	ND	5.5	0.96	6
Metoprolol	ND	44	22	1	6
Mofarotene	ND	130	4.0	0.0	7
Nicardipine	ND	6700	13	0.084	8
Nilvadipine	ND	36000	14	0.013	8
Omeprazole	ND	330	13	0.160	8
Oxodipine	ND	5.3	4.5	1	6
Phenacetin	78	33	21	1	6
Propranolol	1800	4300	25	0.72	12,13
Tacrine	1000	ND	21	1	3
R-warfarin	ND	7	0.13	0.023	3
S-warfarin	ND	2.1	0.046	0.011	3
YM796	ND	870	24	0.694	14
Zolpidem	ND	83	9.1	0.146	8
Alprazolam	33	180	19	0.35	Unpublished observation
Caffeine	1.4	4.3	3.0	1.0	3
Chlordiazepoxide	8.0	4.6	2.5	0.15	Unpublished observation
Clobazam	27	110	7.9	0.21	Unpublished observation
Clonazepam	15	18	4.9	0.21	Unpublished observation
Codeine	290	ND	23	1	6
Dextromethorphan	110	450	20	0.45	15
Diazepam	82	81	17	0.15	3
Diclofenac	110	110	3.6	0.017	16
Ethoxycoumarin (ECOD)	26	50	14	0.22	6
Flunitrazepam	46	89	12	0.25	Unpublished observation
Heptabarbitone	29	ND	16	0.62	6
Heptylbarbitone	33	ND	5.2	0.066	6
Hexobarbitone	ND	330	16	0.62	6
Ibuprofen	ND	29	0.60	0.01	6
Ketoconazole	55	42	6.4	0.062	17
Midazolam	74	81	11	0.07	Unpublished observation
Ondansetron	110	320	15	0.25	3
Phenytoin	37	35	7.0	0.2	3
Tolbutamide	1.6	6.2	0.12	0.08	3
Triazolam	140	130	21	0.28	Unpublished observation
Diazepam in PB treated	120	132	16	0.22	18
ECOD in BNF treated	240	470	22	0.22	3
Diazepam in DEX treated	220	480	16	0.15	3
Diazepam in ABT treated	9.4	7.5	1.2	0.15	Unpublished observation
Diclofenac in ABT treated	34	32	0.77	0.017	Unpublished observation

Compounds in italic letters are those studied in our laboratory. ND: not determined.

Table II. Scaling Factors for Isolated Rat Hepatocytes and Rat Liver Microsomes*

Source of data	Hepatocytes		Microsomes	
	Cellularity (10^6 cells/g liver)	Scaling factor (10^6 cells/SRW)	Recovery ratio (mg protein/g liver)	Scaling factor (mg protein per SRW)
Literature	110	1200	45	500
Untreated	110	1200	60	660
PB-treated	110	1200	46	513
BNF-treated	120	1300	57	629
DEX-treated	130	1400	47	516
ABT-treated	105	1160	74	814

* Refs. 3 and 19.

per SRW (SRW = standard rat weight of 250 g) using the scaling factors shown in Table II.

Using the scaled CL_{int} values, the CL_h and the hepatic availability ($F_h = 1 - CL_h/Q_h$) were predicted based on the following three models using the blood unbound fraction, f_u, for each drug and the hepatic blood flow, Q_h = 25 ml/min per SRW (20,21):

1. Well-stirred model

$$CL_h = \frac{Q_h \cdot f_u \cdot CL_{int}}{Q_h + f_u \cdot CL_{int}}$$

2. Parallel tube model

$$CL_h = Q_h\left[1 - \exp\left(-\frac{f_u \cdot CL_{int}}{Q_h}\right)\right]$$

3. Dispersion model

$$CL_h = Q_h\left[1 - \frac{4a}{(1+a)^2 \exp[(a-1)/2Dn] - (1-a)^2 \exp[-(a+1)/2Dn]}\right]$$

where Dn = 0.17 (4),

$$a = \sqrt{1 + 4RnDn} \text{ and } Rn = \frac{f_u \cdot CL_{int}}{Q_h}$$

On the other hand, *in vivo* CL_{int} values were calculated from the same models using CL_h data reported in the literature or in-house and compared to the predicted CL_{int}.

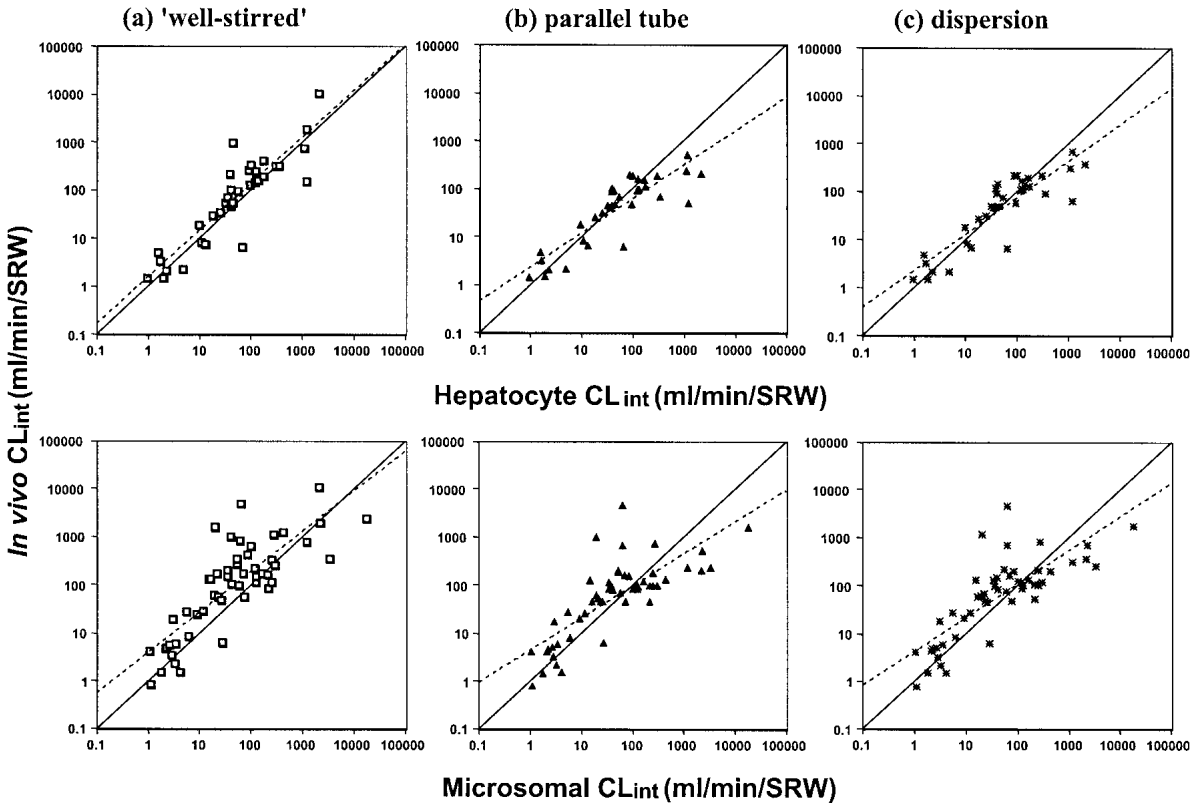

Fig. 1. Correlations between the observed CL_{int} and CL_{int} predicted from rat microsomes and hepatocytes using the (a) "well-stirred," (b) parallel tube, and (c) dispersion models. Lines represent the regression (dotted) and unity (solid).

Two levels of comparisons were made: 1) predicted (scaled *in vitro*) CL_{int} values were compared to *in vivo* CL_{int} values modeled from hepatic clearance, and 2) predicted CL_h (obtained from modeling the scaled *in vitro* CL_{int} values) were compared to *in vivo* CL_h.

Estimation of the Accuracy (Precision and Bias) of Predictions

In order to compare the accuracy of predictions based on the three models, the root mean squared prediction error (*rmse*) and the average fold-error (*afe*) were estimated as measures of precision and bias, respectively, for each set of predictions (22,23). Both measures use the prediction error (difference between predicted and observed *in vivo* values) for each drug in a particular *in vitro* system. The variance of the prediction is calculated from the sum of the squares of the prediction errors and this provides the *rmse.* The geometric mean of the prediction error provides a measure of bias with equal value to under- and overpredictions in the form of *afe*.

$$afe = 10^{\left|\frac{1}{N}\sum \log \frac{\text{Predicted}}{\text{Observed}}\right|}$$

$$mse = \frac{1}{N}\sum (\text{Predicted} - \text{Observed})^2,$$

$$rmse = \sqrt{mse}$$

The correlation analyses were also performed between the predicted and observed values for each parameter and the correlation coefficient squared (r^2) was also used to assess the *in vitro in vivo* relationships. For the clearance parameters (CL_h and CL_{int}), the predicted/observed ratio was also calculated for each drug and displayed on a logarithmic scale in order to give a symmetrical distribution. On these data displays, lines indicating both the 2-fold (log ratio –0.3 and 0.3) and 3-fold (log ratio –0.5 and 0.5) error on the perfect prediction (log ratio 0) of CL_{int} are shown. These plots were used to obtain the percentage of predictions within particular bands.

RESULTS

The relationships between the CL_{int} predicted from rat microsomes and hepatocytes and the *in vivo* observed CL_{int} calculated from either the "well-stirred," parallel tube, or dispersion models are presented in Fig. 1. The statistical comparisons of these predictions are summarized in Table III. In general, predictions from hepatocyte data are more precise (lower *rmse*) and less biased (lower *afe*) with higher r^2 values than from the microsomal data. Also the log of the ratio of the predicted/observed CL_{int} (Fig. 2) indicates a lower percentage of predictions falling outside the 2-fold error (34–40%) for the hepatocyte than for the microsomal prediction (62–67%).

For the microsomal prediction, the parallel tube and dispersion models showed less bias than the "well-stirred" model but the precision was similar for all three models. For the hepatocyte data, there was little difference in the bias between the models but more precision in the parallel tube and dispersion models relative to the "well-stirred" model. The log of the ratio of the predicted/observed CL_{int} (Fig. 2), for a particular *in vitro* system, indicates similar percentage of predictions falling outside the 2-fold error irrespective of the liver model used. However, in the case of the parallel tube and dispersion models, these are overpredictions of high CL_{int} values.

Overall, the CL_{int} predictions based on the parallel tube and dispersion models (Figs. 1b and 1c, Figs. 2b and 2c) are similar to each other (Table III). Also, the predicted-observed relationship for both the parallel tube and dispersion models exhibit a degree of curvature tending toward the higher clearance drugs for both the hepatocyte and microsomal predictions.

When hepatic clearance is considered, the correlations between observed and predicted values using the 3 liver models (Figs. 3a–3c) also demonstrate a greater extent of scatter around the line of unity for microsomes compared to hepatocytes, with a greater degree of underprediction from the microsomal data. Similar to the prediction of CL_{int}, hepatocytes produce a more accurate prediction of CL_h with less bias and more precision (Table III). Visually (Fig. 3), the "well-stirred" model gives poorer prediction of CL_h than the parallel tube or dispersion models, both of which demonstrate similar trends. This is also evident in the plot of the ratio of predicted/observed hepatic clearance (Fig. 4), particularly for microsomes in the low CL_h region. However, with both *in vitro* systems, the difference in the statistical estimates of bias and precision for the CL_h prediction from the three models were only marginal.

Table III. Statistical Data Comparing the Accuracy of Predictions

	Hepatocyte prediction			Microsomal prediction		
	Well-stirred	Parallel tube	Dispersion	Well-stirred	Parallel tube	Dispersion
CL_{int}						
afe	1.41	1.26	1.12	2.14	1.28	1.43
rmse	1405	433	400	2581	2424	2401
r^2	0.792	0.737	0.762	0.667	0.601	0.625
% outside 2-fold error	37	40	34	67	61	65
CL_h						
afe	1.16	1.03	1.06	1.70	1.54	1.58
rmse	3.49	3.21	3.15	5.14	5.09	5.11
r^2	0.864	0.879	0.877	0.693	0.708	0.700
F_h						
afe	1.22	35.57	2.39	1.26	6.86	1.62
rmse	0.140	0.129	0.126	0.205	0.204	0.204
r^2	0.864	0.879	0.877	0.693	0.708	0.700

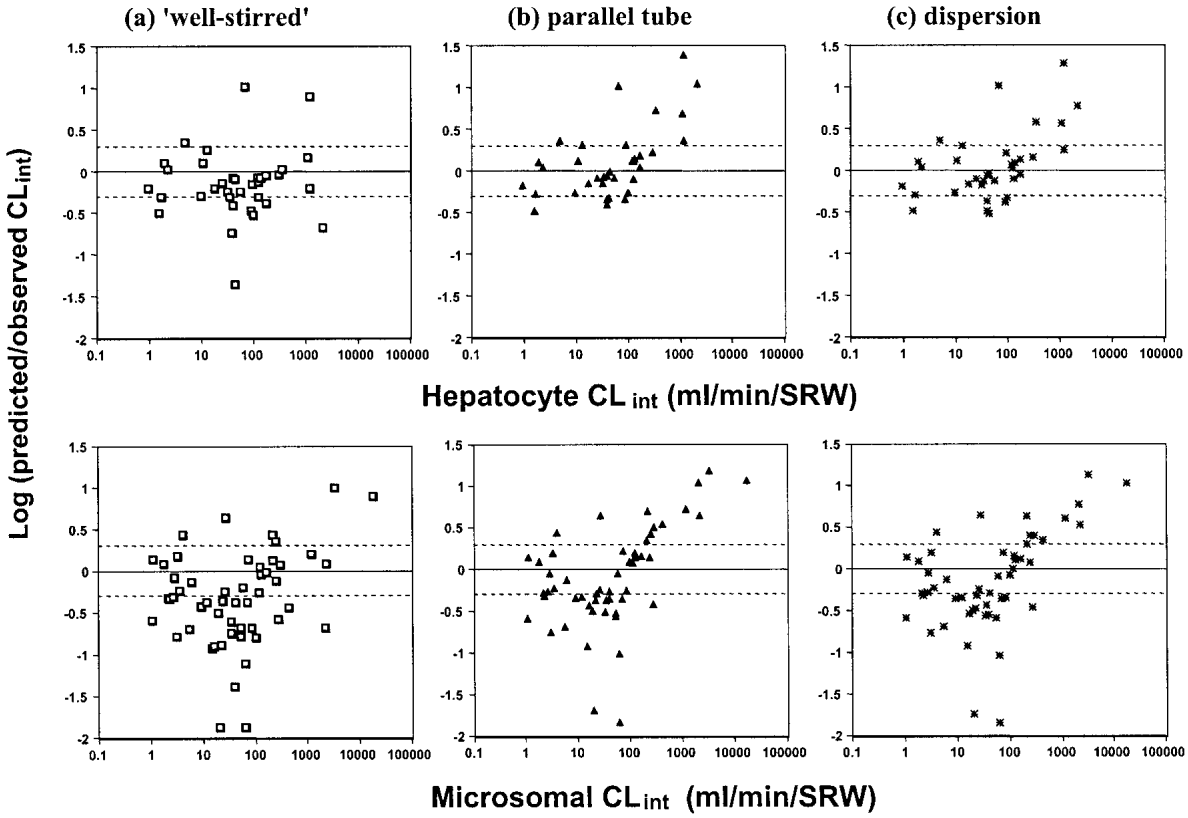

Fig. 2. Relationship between the log predicted/observed CL_{int} ratio and CL_{int} predicted from rat microsomes and hepatocytes using the (a) "well-stirred," (b) parallel tube, and (c) dispersion models. Lines represent the limits at half and double the observed value.

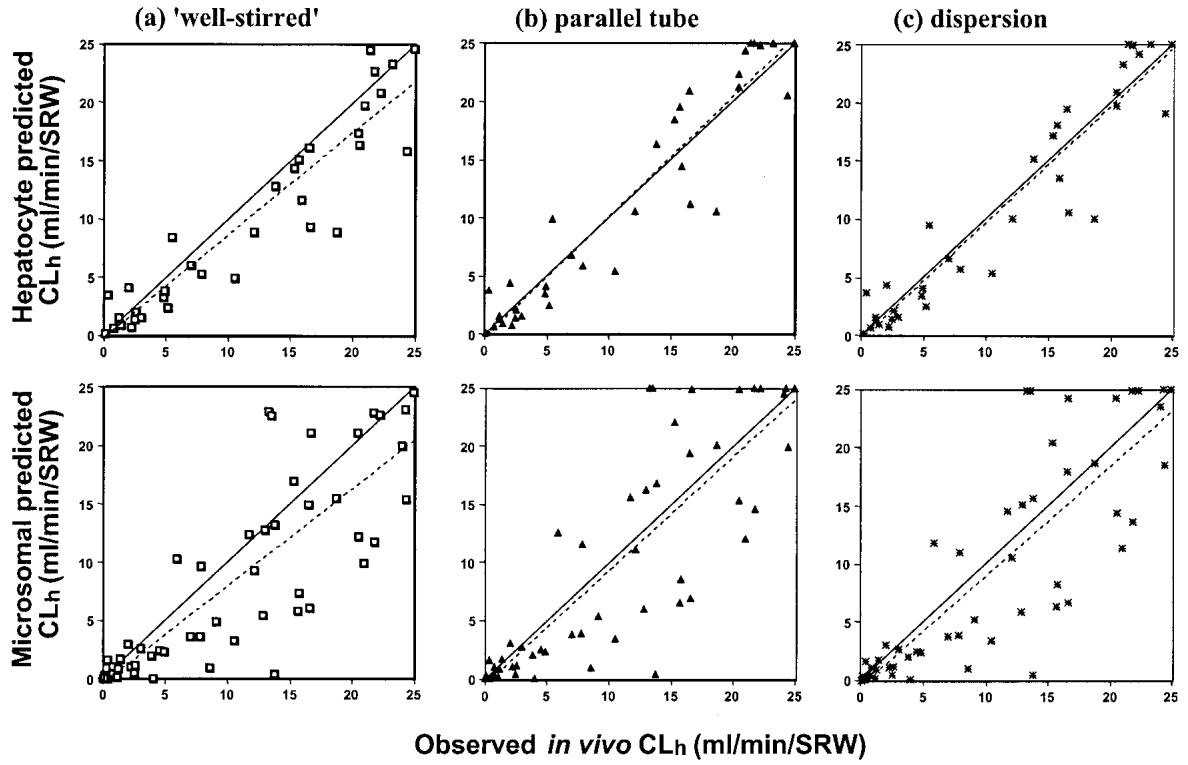

Fig. 3. Correlations between the observed CL_h and CL_h predicted from rat microsomes and hepatocytes using the (a) "well-stirred," (b) parallel tube, and (c) dispersion models. Lines represent the regression (dotted) and unity (solid).

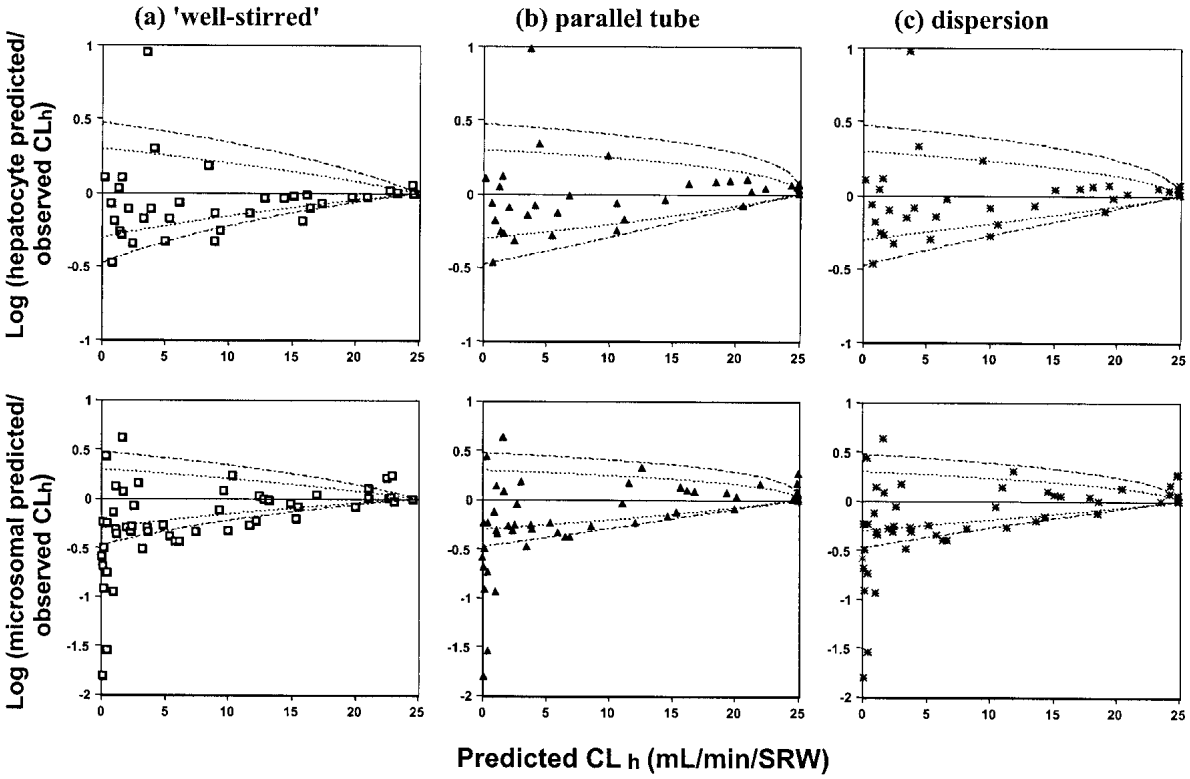

Fig. 4. Relationship between the log of the predicted/observed CL_h ratio and the predicted CL_h for microsomes and hepatocytes using the (a) "well-stirred," (b) parallel tube, and (c) dispersion models. The dashed lines show the propagation of a 2- and 3-fold error in CL_{int} in the hepatic clearance prediction.

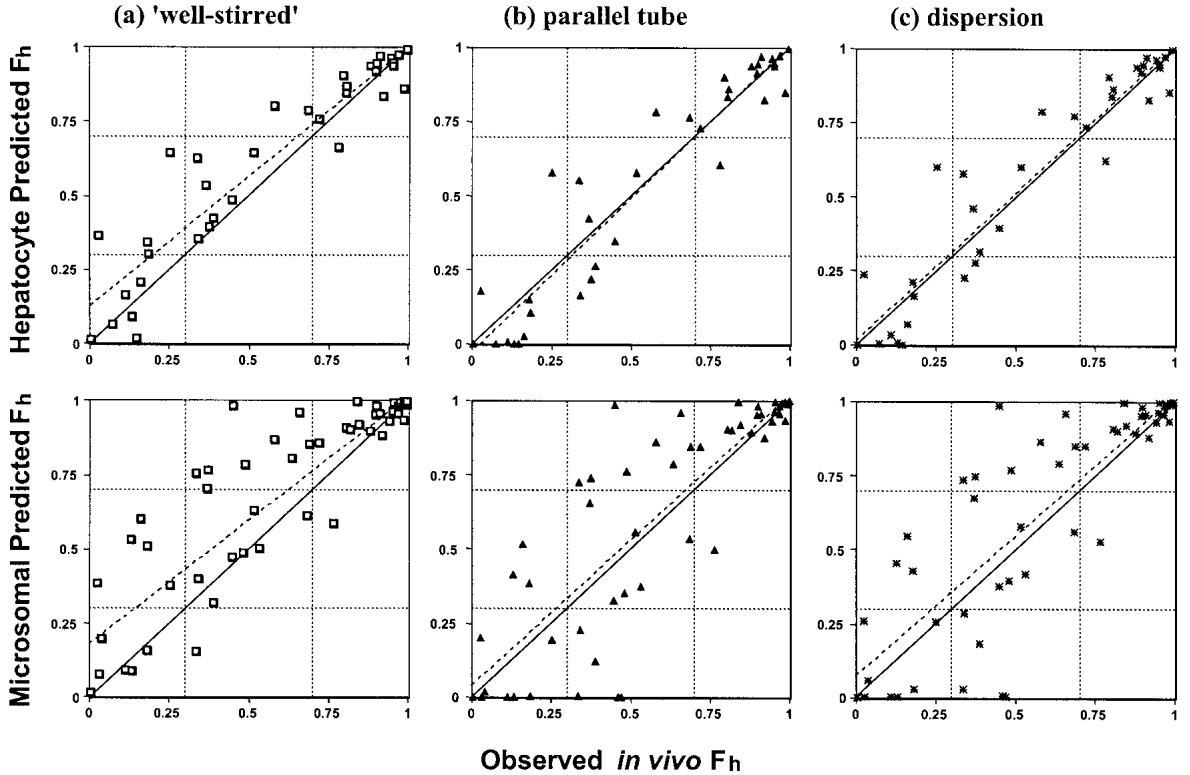

Fig. 5. Correlations between the observed F_h and F_h predicted from rat microsomes and hepatocytes using the (a) "well-stirred," (b) parallel tube, and (c) dispersion models. Lines represent the regression (dotted) and unity (solid).

Similar results were obtained for the prediction of F_h in that the "well-stirred" model overpredicted to a greater extent than the other two models (Fig. 5).

DISCUSSION

Given the destructive nature of the preparation of liver microsomes, resulting in the loss of both cellular integrity and most of the non–cytochrome P450 drug metabolizing enzymes, it is often assumed that hepatocytes will potentially give better prediction of metabolic stability. This premise appears to be true as comparisons of these two systems show that rat hepatocytes produce consistently more accurate and precise predictions of both CL_{int} and CL_h compared to microsomes irrespective of the liver model applied. Thus, it can be concluded that hepatoctyes provide a better system for evaluating these liver models. Previous evaluations (4,5) have been limited to hepatic microsomal comparisons.

The current analysis considers an evaluation of the *in vitro* CL_{int} values relative to *in vivo* CL_{int} values obtained from "deconstructing" CL_h with the use of the three liver models. This academic view generates the widest range of parameter values (4 orders of magnitude) to allow *in vitro-in vivo* comparisons. Also considered are the CL_h parameters obtained from each of the liver models using the *in vitro* CL_{int} values. This pragmatic approach does not allow such detailed *in vitro-in vivo* comparisons of enzyme activity but, by incorporating the processes of drug binding and hepatic blood flow, it desensitizes the scaling process to inaccuracies at the high end of enzyme activity.

When CL_{int} values from *in vitro* and *in vivo* are compared it is clear that the simpler "well-stirred" model gave the poorest predictions, and there is nothing to distinguish the dispersion and parallel tube models. Considering the mathematical complexity of the dispersion model, it is recommended that the parallel tube model be used in preference to the "well-stirred" model for the prediction of *in vivo* CL_{int}. There is general agreement for all models that the extensive 4-order range of enzyme activity reported in both hepatic microsomes and hepatocytes is a true reflection of the *in vivo* situation. It is of interest that the predicted vs. observed CL_{int} relationship for both the parallel tube and dispersion models exhibit a degree of curvature tending toward the higher clearance drugs for both the hepatocyte and microsomal predictions. This may be attributed to the inability of the *in vitro* systems to reflect a permeability limitation that will occur *in vivo* (24).

For CL_h predictions from the three liver models using either hepatocyte or microsomal parameters, it is less apparent whether one particular model offers any advantages over another. Table III shows that the statistical estimates of bias and precision for the CL_h prediction show minor differences between the models. Therefore, the common practice of using the "well-stirred" model would appear to be quite satisfactory. Certainly for screening procedures to identify new chemical entities with low CL_h (or high F_h) *in vivo*, the "well-stirred" model can be incorporated into prediction algorithms without concern.

REFERENCES

1. J. H. Lin and A. Y. Lu. Role of pharmacokinetics and metabolism in drug discovery and development. *Pharmacol. Rev.* **49**:403–449 (1997).
2. R. S. Obach. Prediction of human clearance of twenty-nine drugs from hepatic microsomal intrinsic clearance data: An examination of *in vitro* half-life approach and nonspecific binding to microsomes. *Drug Metab. Dispos.* **27**:1350–1359 (1999).
3. J. B. Houston and D. J. Carlile. Prediction of hepatic clearance from microsomes, hepatocytes, and liver slices. *Drug Metab. Rev.* **29**:891–922 (1997).
4. M. Roberts and M. Rowland. Correlation between in-vitro microsomal enzyme activity and whole organ hepatic elimination kinetics: analysis with a dispersion model. *J. Pharm. Pharmacol.* **38**:177–181 (1986).
5. Y. Sugiyama, Y. Sawada, T. Iga, and M. Hanano. Reconstruction of in vivo metabolism from in vitro data. In R. Kato, R. W. Estabrook, and M. N. Cayen (eds.), *Xenobiotic Metabolism & Disposition; Proceedings of the 2nd International ISSX Meeting,* Taylor & Francis, London, 1989, pp. 225–235.
6. J. B. Houston. Utility of *in vitro* drug metabolism data in predicting *in vivo* metabolic clearance. *Biochem. Pharmacol.* **47**: 1469–1479 (1994).
7. T. Lave, S. Dupin, C. Schmitt, R. C. Chou, D. Jaeck, and P. Coassolo. Integration of *in vitro* data into allometric scaling to predict hepatic metabolic clearance in man: Application to 10 extensively metabolized drugs. *J. Pharm. Sci.* **86**:584–590 (1997).
8. Y. Naritomi, S. Terashita, S. Kimura, A. Suzuki, A. Kagayama, and Y. Sugiyama. Prediction of human hepatic clearance from *in vivo* animal experiments and *in vitro* metabolic studies with liver microsomes from animals and humans. *Drug Metab. Dispos.* **29**: 1316–1324 (2001).
9. M. Chiba, M. Hensleigh, and J. H. Lin. Hepatic and intestinal metabolism of indinavir, an HIV protease inhibitor, in rat and human microsomes. Major role of CYP3A. *Biochem. Pharmacol.* **53**:1187–1195 (1997).
10. J. H. Lin, M. Chiba, S. K. Balani, I.-W. Chen, G. Y.-S. Kwei, K. J. Vastag, and J. A. Nishime. Species differences in the pharmacokinetics and metabolism of indinavir, a potent human immunodeficiency virus protease inhibitor. *Drug Metab. Dispos.* **24**: 1111–1120 (1996).
11. T. Prueksaritanont, S. K. Balani, L. M. Dwyer, J. D. Ellis, L. R. Kauffman, S. L. Varga, S. M. Pitzenberger, and A. D. Theoharides. Species differences in the metabolism of a potent HIV-1 reverse transcriptase inhibitor L-738,372: In vivo and in vitro studies in rats, dogs, monkeys, and humans. *Drug Metab. Dispos.* **23**:688–695 (1995).
12. R. Ishida, S. Obara, Y. Masubuchi, S. Narimatsu, S. Fujita, and T. Suziki. Induction of propranolol metabolism by the azo dye sudan III in rats. *Biochem. Pharmacol.* **43**:2489–2492 (1992).
13. D. B. Jones, M. S. Ching, R. A. Smallwood, and D. J. Morgan. A carrier-protein receptor is not a prerequisite for avid hepatic elimination of highly bound compounds: A study of propranolol elimination by the isolated perfused rat liver. *Hepatology* **5**:590–593 (1985).
14. T. Iwatsubo, H. Suzuki, and Y. Sugiyama. Prediction of species differences (rats, dogs, humans) in the *in vivo* metabolic clearance of YM796 by the liver from *in vitro* data. *J. Pharmacol. Exp. Ther.* **283**:462–469 (1997).
15. L. E. Witherow and J. B. Houston. Sigmoidal kinetics of CYP3A substrates: an approach for scaling dextromethorphan metabolism in hepatic microsomes and isolated hepatocytes to predict in vivo clearance in rat. *J. Pharmacol. Exp. Ther.* **290**:58–65 (1999).
16. A. J. Stevens, S. W. Martin, B. S. Brennan, A. McLachlan, L. A. Gifford, M. Rowland, and J. B. Houston. Regional drug delivery II: relationship between drug targeting index and pharmacokinetic parameters for three non-steroidal anti-inflammatory drugs using the rat air pouch model of inflammation. *Pharm. Res.* **12**: 1987–1996 (1995).
17. D. Matthew, B. Brennan, K. Zomorodi, and J. B. Houston. Disposition of azole antifungal agents. I. Nonlinearities in ketoconazole clearance and binding in rat liver. *Pharm. Res.* **10**:418–422 (1993).
18. D. J. Carlile, K. Zomorodi, and J. B. Houston. Scaling factors to relate drug metabolic clearance in hepatic microsomes, isolated hepatocytes, and the intact liver: studies with induced livers involving diazepam. *Drug Metab. Dispos.* **25**:903–911 (1997).
19. D. J. Carlile, N. Hakooz, and J. B. Houston. Kinetics of drug

metabolism in rat liver slices: IV. Comparison of ethoxycoumarin clearance by liver slices, isolated hepatocytes, and hepatic microsomes from rats pretreated with known modifiers of cytochrome P-450 activity. *Drug Metab. Dispos.* **27**:526–532 (1999).
20. G. M. Pollack, K. L. R. Brouwer, K. B. Demby, and J. A. Jones. Determination of hepatic blood flow in the rat using sequential infusions of indocyanine green or galactose. *Drug Metab. Dispos.* **18**:197–202 (1999).
21. K. S. Pang and J. R. Gillette. Compications in the estimation of hepatic blood flow in vivo by pharmacokinetic parameters. *Drug Metab. Dispos.* **6**:567–576 (1978).
22. R. S. Obach, J. G. Baxter, T. E. Liston, B. M. Silber, B. C. Jones, F. MacIntyre, D. J. Rance, and P. Wastall. The prediction of human pharmacokinetic parameters from preclinical and in vitro metabolism data. *J. Pharmacol. Exp. Ther.* **283**:46–58 (1997).
23. L. B. Sheiner and S. L. Beal. Some suggestions for measuring predictive performance. *J. Pharmacokin. Biopharm.* **9**:503–512 (1981).
24. S. Miyauchi, Y. Sawada, T. Iga, M. Hanano, and Y. Sugiyama. Comparison of the hepatic uptake clearances of fifteen drugs with a wide range of membrane permeabilities in isolated rat hepatocytes and perfused rat livers. *Pharm. Res.* **10**:434–440 (1993).